SAND2013-3455C

Nanoantenna-Enabled Midwave Infrared Detection

David W. Peters*, Darin Leonhardt, Charles M. Reinke, Jin K. Kim, Joel R. Wendt, Paul S. Davids, John F. Klem
Sandia National Laboratories, P.O. Box 5800, Albuquerque, NM, USA 87185-1082

ABSTRACT

We show simulation results of the integration of a nanoantenna in close proximity to the active material of a photodetector. The nanoantenna allows a much thinner active layer to be used for the same amount of incident light absorption. This is accomplished through the nanoantenna coupling incoming radiation to surface plasmon modes bound to the metal surface. These modes are tightly bound and only require a thin layer of active material to allow complete absorption. Moreover, the nanoantenna impedance matches the incoming radiation to the surface waves without the need for an antireflection coating. While the nanoantenna concept may be applied to any active photodetector material, we chose to integrate the nanoantenna with an InAsSb photodiode. The addition of the nanoantenna to the photodiode requires changes to the geometry of the stack beyond the simple addition of the nanoantenna and thinning the active layer. We will show simulations of the electric fields in the nanoantenna and the active region and optimized designs to maximize absorption in the active layer as opposed to absorption in the metal of the nanoantenna. We will review the fabrication processes.

Keywords: Midwave, infrared, focal plane array, detector, plasmon, nanoantenna

1. INTRODUCTION

Improved infrared detector performance is always a demand from end users. Nanoantennas are an enabling technology for visible to terahertz components and may be used with a variety of detector materials. In the work described here, we design and fabricate nanoantennas integrated with proven InAsSb detector technology. Nanoantennas offer a means to make infrared detectors much thinner, thus lowering the dark current and improving performance. The nanoantenna is the enabling component of these thin devices, and its incorporation with the detector material is the primary challenge. The nanoantenna is a subwavelength periodic structure; several periods are contained in each linear dimension for each array pixel.

Whereas a traditional detector needs to be several microns thick to fully absorb an incident plane wave, a nanoantenna-enabled detector can use a much thinner layer of active material. This is the result of the concentration of energy in surface waves. The surface waves are concentrated in a small volume directly under the nanoantenna surface. Thus, the active layer only needs to contain the volume of these enhanced electric fields.

Even with the collection of every photon (none reflected), the performance of a traditional detector at low photon flux may be limited by noise associated with detector dark current. The reduction of the active layer volume by over an order of magnitude is what allows the detector to have a lower dark current, or operate at higher temperatures for the same dark current. Furthermore, it allows more flexibility in the amount of strain in the materials, thus allowing the cutoff wavelength to be tuned to a larger extent than in thicker layers.

The nanoantenna converts incident plane waves into surface waves at the metal interface. These surface modes conduct energy around the metal surface to the backside of the patterned metal. Here the energy may be converted by the active material to carriers. An example nanoantenna is shown in Figure 1 along with the electric field that can be seen to conform to the metal surface. The nanoantenna consists of a top patterned metal layer, the active material and other semiconductor layers, and a back metal ground plane. By sandwiching the active material between a patterned metal layer and a metal back plane, the metal for the two contacts of the pixel are readily available.

The shape and dimensions of the nanoantenna determine the spectral and polarization passband. The pattern is defined lithographically and is therefore easily changed from pixel to pixel. This allows the detector to perform functions now performed with external polarizers or filters, albeit with decreased resolution.

* dwpeter@sandia.gov

At the design wavelength, the nanoantenna has a broad angular band where the reflection is near zero.[1] This allows us to design a detector structure without the need for antireflection coatings on the detector surface. This becomes increasingly important for an array in which different pixels respond to different spectral bands. The nanoantenna at each pixel is optimized for that band, and thus zero reflection can be achieved at every pixel irrespective of the wavelength it is collecting. This is impossible to implement in a practical way with thin films, where a single compromise coating is applied across all pixels. Moreover, the wavelength band of the nanoantenna passband does not change with angle. This allows the collection of the same passband over a broad angular range, for example if the array has light focused onto it by an f/1 optic. With thin films there is generally a corresponding change in the passband with a change in angle.

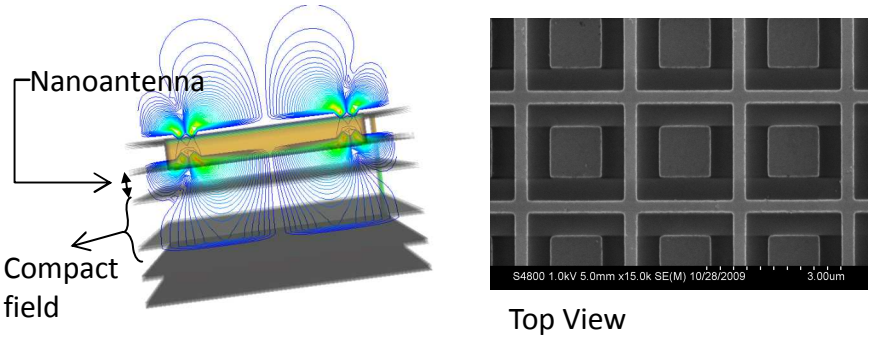

Figure 1. Illustration of a midwave infrared FPA pixel utilizing a nanoantenna. The nanoantenna allows over an order of magnitude reduction in the required thickness of the active layer.

Here we will describe the design process and steps in the fabrication process. This includes the design of the nanoantenna parameters to maximize the optical absorption in the active layer, fabrication processes, and wafer removal and bonding studies.

2. OPTICAL DESIGN

The optical design of the nanoantenna structures is accomplished using a suite of electromagnetic codes. Rigorous coupled wave analysis (RCWA) is used to determine the location and magnitude of the absorption peak. A square loop design common in RF frequency selective surface (FSS) work was chosen for its broader bandwidth. Using RCWA, we vary the period and relative width of the outer gold lines, aperture, and central gold square of the nanoantenna. We then take promising designs from the RCWA simulations and use either finite difference time domain (FDTD) or finite-element modeling (FEM) simulations to better understand where the absorption is occurring in the structures. Understanding the spatial dependence of absorption is important as absorption can occur in the gold nanoantenna, non-transparent semiconductor layers, and the bottom metal ground plane, as well as the desired absorption in the active layer.

This approach allows us to optimize the detector and nanoantenna parameters to maximize the energy absorbed in the active layer. The layer structure of the epitaxially grown semiconductor stack may be varied, but only within boundaries set by practical considerations, such as the need for certain minimum thicknesses in some layers to act as barriers for metal diffusion. Lateral dimensions of the nanoantenna patterned metal layer are limited by the minimum resolvable feature size obtained lithographically. Given these limitations, we want to maximize the absorption in the active layer where carriers are generated and not in the other layers where only phonons are generated. The stack used for the modeling and fabrication of these detectors is shown in Figure 2. In this particular case the superstrate is assumed to be silicon nitride. This allows the nanoantenna and detector to be interrogated through a transparent handler wafer to be described in greater detail in the fabrication section.

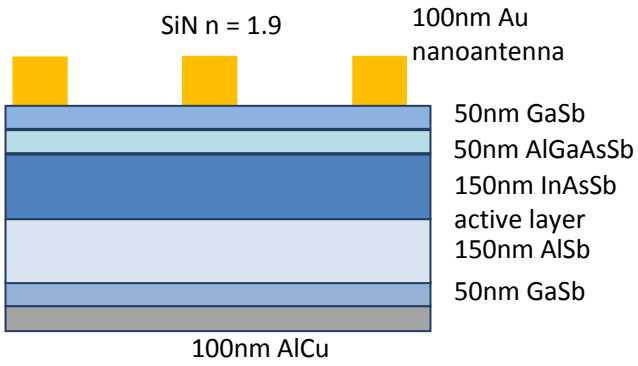

Figure 2. Epitaxial layers sandwiched between lower metal ground plane and upper patterned nanoantenna layer.

Three designs of possible single unit cells of the periodic nanoantenna are shown in Figure 3. The use of silicon nitride leads to smaller unit cell dimensions for the nanoantenna as a result of the higher index of refraction (n ~ 1.9) above the patterned gold layer. Note that the outer metal grid dimensions lead to gold lines of twice those dimensions as the unit cells are replicated periodically.

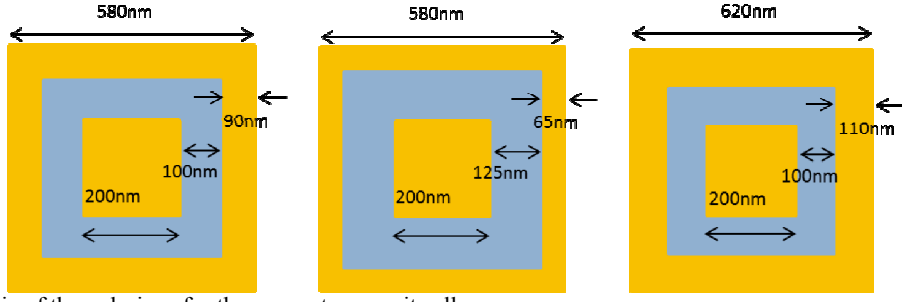

Figure 3. Schematic of three designs for the nanoantenna unit cell.

This unit cell is used in RCWA, FDTD, and FEM modeling using periodic boundary conditions. The top nanoantenna layer and bottom metal contact are assumed to be gold and aluminum/copper respectively. The RCWA results for the absorption at normal incidence are shown in Figure 4. As the designs are x-y symmetric there is no difference in polarization response.

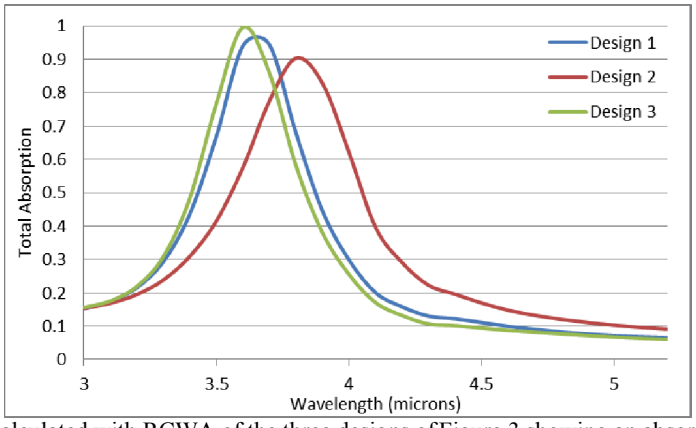

Figure 4. Total absorption as calculated with RCWA of the three designs of Figure 3 showing an absorption peak for each design in the MWIR.

The RCWA simulations give us the total absorption in the structure, however the absorption that occurs in the metal is undesirable. We therefore need to determine exactly where the absorption occurs. For this we use an FEM code and individually look at the absorption in each layer of the device. This code also lets us look at the field plots to determine where high field regions exist in the structure. We show a sample breakdown of this absorption in Figure 5. The total absorption is the sum of these curves. We note that the resonance is slightly red shifted from the RCWA simulations. The curve labeled "absorber" shows the absorption that occurs in the active layer of the device. This absorption occurs just before the cut-off of the material at wavelengths longer than 4.1μm. The labels "outer Au" and "inner Au" refer to losses in the outer metal Au mesh and the inner gold square of the patterned nanoantenna. We note that the majority of the unwanted absorption in this design occurs in the continuous gold mesh formed by the outer edge of the nanoantenna unit cell. Optimization of the structure will increase the ratio of the absorption in the active layer compared to the absorption in the lower and upper metal layers.

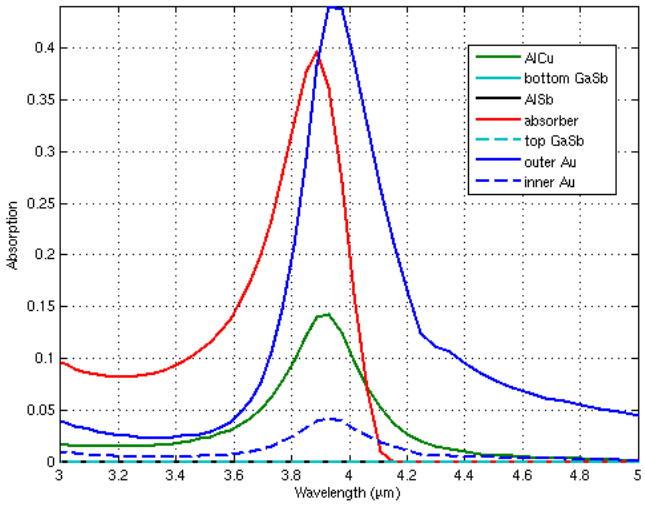

Figure 5. Total absorption of the design 1 of Figure 3 showing the absorption in each layer of the structure.

3. FABRICATION

Integration of the nanoantenna in close proximity to the active absorber layer presents several fabrication challenges. One fabrication process involves patterning the nanoantenna first. This ensures a flat, unadulterated surface for the e-beam processing.

For nanoantenna-first processing, the expitaxial layers are grown on a GaSb substrate in reverse order compared to the normal sequence for detector epitaxial layer design. The epilayers include a 100nm InAsSb etch stop layer, 50nm p-type GaSb contact layer, 100nm $AlGa_{0.15}AsSb$ electron barrier, 100nm InAsSb absorber, and a 50nm $AlGa_{0.15}AsSb$ absorber passivation layer. We have found that adding 15% Ga to the wide gap AlAsSb is effective in preventing oxidation of the layer when exposed to air. The absorber layer is near the surface, covered only by a thin, unintentionally doped wide-band gap semiconductor that acts as a surface passivation for the absorber. The passivation layer is critical for a thin absorber where surface/interface generation/recombination effects can dominate the detector performance.

Next, the nanoantenna pattern is created on the surface of the passivation layer using a combination of e-beam lithography and subsequent metal deposition and liftoff. The nanoantenna is encapsulated with silicon nitride to provide a uniform refractive index and to promote the adhesion of benzocyclobutene (BCB), which is spin-coated onto the nitride. A handle wafer of sapphire is also coated with nitride and BCB and bonded to the BCB coating on the nanoantenna sample.

We have found that the BCB must be fully cured in nitrogen ambient during the bonding process so that the bonded epilayers remain flat and stable after substrate removal. If the BCB is not fully cured, the epitaxial layers develop

buckling and delamination during subsequent processing steps. Additionally, bubbles may form in the BCB, as shown in Figure 6. However, the nanoantenna metal can potentially spike through the thin passivation layer and contaminate the absorber at the elevated temperatures required during the BCB cure. We have found that a thin layer of Ti beneath the Au of the nanoantenna and above the $AlGa_{0.15}AsSb$ passivation layer is effective in preventing Au from reacting with the passivation layer during the BCB bonding process.

Once the sample is successfully bonded to the sapphire handle wafer, the GaSb substrate is thinned down to 50μm using lapping/polishing. The remainder is chemically etched in a solution of 1 part 1M CrO_3 to 2 parts 100:1 de-ionized (DI) H_2O:HF (49 wt. %). The substrate etch selectively stops on an InAsSb sacrificial layer. The InAsSb is then selectively removed in a 1:1 solution of citric acid:H_2O_2 (30wt. %). The citric acid solution is made by mixing 1g anhydrous citric acid per 1ml DI. The etch terminates on the GaSb cap layer, where fabrication of detectors begins.

Detectors are fabricated using a mesa etch isolation process which terminates on the $AlGa_{0.15}AsSb$ barrier layer. Thus, the absorber surface is passivated at both interfaces by $AlGa_{0.15}AsSb$. Testing of the detectors is made more difficult by the inability to wirebond to the top contact of the detectors. We find that the ball-and-wedge bonding process results in tearing of the metal pad. Apparently, this problem results from the delicate condition of the epilayers bonded with the BCB. Therefore, we are currently pursuing alternative designs to circumvent the problem of wirebonding directly to the detectors.

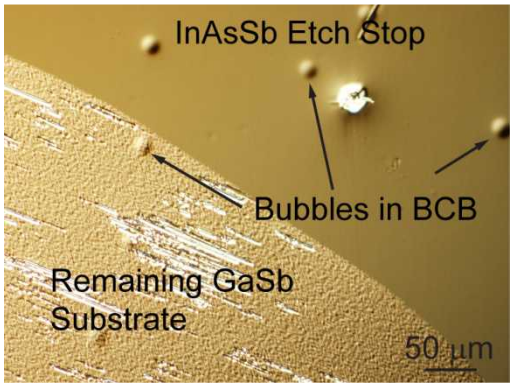

Figure 6. Nomarski optical micrograph showing the partial removal of the GaSb substrate. The BCB was not fully cured resulting in the formation of bubbles beneath the surface of the epitaxial layers.

4. CONCLUSIONS

Infrared detector performance can be enhanced through the use of nanoantenna devices in the form of a subwavelength patterned metal surface. This broad area metal nanoantenna completely covers the pixel face, converting incident radiation to bound surface modes. These highly confined modes allow us to greatly thin the active layer of the detector, thus reducing the dark current. Moreover, the nanoantenna offers optical filtering features such as polarimetry and spectral selectivity that may be varied pixel to pixel.

The design of the detector layers and the lateral dimensions of the nanoantenna require optimization to maximize the absorption in the active layer. In the example of this paper, we use an nBn InGaAs detector. The fabrication of the detector layers and nanoantenna are not the same as for a traditional detector, requiring close cooperation between fabrication and modeling efforts.

The fabrication process involves writing the nanoantenna early in the fabrication process, immediately after growth of the epitaxial layers. The bonded wafer process we use is described, allowing the thin epi layer to be separated from its original GaSb substrate on which it was grown. Benzocyclobutene is used as an adhesion layer of the epitaxial layers to the sapphire handler wafer to be used for the characterization phase.

ACKNOWLEDGEMENT

Sandia National Laboratories is a multi-program laboratory managed and operated by Sandia Corporation, a wholly owned subsidiary of Lockheed Martin Corporation, for the U.S. Department of Energy's National Nuclear Security Administration under contract DE-AC04-94AL85000.

REFERENCES

[1] Peters, D.W., Davids, P., Wendt, J.R., Cruz-Cabrera, A.A., Kemme, S.A. and Samora, S., "Metamaterial-inspired high-absorption surfaces for thermal infrared applications," Proc. SPIE 7609, 76091C (2010).